Molecular Dynamics Simulations of the Mononuclear Zinc-β-lactamase from *Bacillus cereus* Complexed with Benzylpenicillin and a Quantum Chemical Study of the Reaction Mechanism

Natalia Díaz,[‡] Dimas Suárez,[†,§] and Kenneth M. Merz, Jr.*[,§]

Contribution from the Departamento de Química Física y Analítica, Universidad de Oviedo, Julián Clavería 8, 33006 Oviedo, Asturias, Spain, and 152 Davey Laboratory, Department of Chemistry, The Pennsylvania State University, University Park, Pennsylvania 16802-6300

Received May 30, 2001

Abstract: Herein, we present results from MD simulations of the Michaelis complex formed between the *B. cereus* zinc-β-lactamase enzyme and benzylpenicillin. The structural and dynamical effects induced by substrate-binding, the specific role of the conserved residues, and the near attack conformers of the Michaelis complex are discussed. Quantum chemical methods (HF/6-31G* and B3LYP/6-31G*) are also applied to study the hydrolysis reaction of *N*-methylazetidinone catalyzed by a monozinc system consisting of the side chains of the histidine residues (His86, His88, and His149) complexed with Zn−OH and the side chains of Asp90 and His210. From this model system, we built molecular-mechanics representations of the prereactive complex and transition state configurations docked into the active site. Linear-scaling semiempirical calculations coupled with a continuum solvent model were then performed on these static models. We propose that the experimental rate data for the *B. cereus* enzyme is compatible with a one-step mechanism for the hydrolysis of β-lactam substrates in which His210 acts as a proton donor.

Introduction

Bacteria develop antibiotic-resistance strategies in three major ways: production of hydrolytic enzymes known as β-lactamases, changes in the permeability of the cell membrane, and alterations of the target enzymes. Among these mechanisms, β-lactamase production is generally considered as the primary route of resistance to β-lactam antibiotics.[1] In particular, zinc-β-lactamases[2] have become a major problem given that these enzymes efficiently hydrolyze nearly all β-lactams including the versatile broad-spectrum antibacterial carbapenem derivatives.[3,4] Moreover, the most widely used inhibitors of serine β-lactamases are also destroyed by these enzymes.[5] Therefore, it is widely accepted that emergence of antibiotic resistance mediated by zinc-β-lactamases comprises an increasing challenge to the therapeutic future of β-lactam antibiotics.

The active site of the zinc-β-lactamases has the potential to bind two zinc(II) ions although their binding affinity for the zinc ions can be quite different: the *Bacillus cereus* enzyme has one high affinity and one low affinity zinc(II) binding site[6] whereas the enzymes from *Bacteroides fragilis*[7] and *Stenotrophomonas maltophilia*[8] bacteria present two high affinity zinc(II) binding sites. Nevertheless, for the *B. cereus* and the *B. fragilis* enzymes, it has been shown that the catalytic efficiency of the dinuclear enzymes is only marginally superior to that of the mononuclear form with some substrates and is even lower with other ones.[9,10] As a result of this fact, some authors have suggested that the mononuclear form of the zinc-β-lactamases would be the predominant form in vivo, where the zinc(II) concentration is expected to be significantly lower with respect to that during enzyme production.[9] Similarly, in experimental studies of functional mimics of zinc-β-lactamases, it has been observed that mononuclear complexes are as reactive in β-lactam hydrolysis as the dinuclear complexes.[11] However, other authors have argued that the presence of the second zinc ion in the *B. fragilis* enzyme represents a genuine evolution of the catalytic mechanism over the *B. cereus* enzyme.[12] It can be concluded, therefore, that obtaining a global theoretical view of the structure and mechanism of zinc-β-lactamases will require the investigation of both the mono- and dizinc forms of these enzymes.

[‡] Universidad de Oviedo.
[§] The Pennsylvania State University.
[†] On leave from Departamento de Química Física y Analítica, Universidad de Oviedo.

(1) Waley, S. G. *β-lactamases: Mechanism of Action*; Page, M. I., Ed.; Blackie Academic&Professional: London, 1992; pp 199−227.
(2) Wang, Z.; Fast, W.; Valentine, A. M.; Benkovic, S. J. *Curr. Opin. Chem. Biol.* **1999**, *3*, 614−622.
(3) Bush, K. *Clin. Infect. Dis.* **1998**, S48−53.
(4) Livermore, D. M.; Woodford, N. *Curr. Opin. Microbiol.* **2000**, *3*, 489−495.
(5) Prosperi-Meys, C.; Llabres, G.; de Seny, D.; Paul-Soto, R.; Hernández-Valladares, M.; Laraki, N.; Frère, J. M.; Galleni, M. *FEBS Lett.* **1999**, *443*, 109−111.
(6) Orellano, E. G.; Girardini, J. E.; Cricco, J. A.; Ceccarelli, E. A.; Vila, A. J. *Biochemistry* **1998**, *37*, 10173−10180.
(7) Crowder, M. W.; Wang, Z.; Franklin, S. L.; Zovinka, E. P.; Benkovic, S. J. *Biochemistry* **1996**, *35*, 12126−12132.
(8) Ullah, J. H.; Walsh, T. R.; Taylor, I. A.; Emery, D. C.; Verma, C. S.; Gamblin, S. J.; Spencer, J. *J. Mol. Biol.* **1998**, *284*, 125−136.
(9) Paul-Soto, R.; Bauer, R.; Frère, J. M.; Galleni, M.; Meyer-Klauche, W.; Nolting, H.; Rossolini, G. M.; de Seny, D.; Hernández-Valladares, M.; Zeppezauer, M.; Adolph, H. W. *J. Biol. Chem.* **1999**, *274*, 13242−13249.
(10) Paul-Soto, R.; Hernández-Valladares, M.; Galleni, M.; Bauer, R.; Zeppezauer, M.; Frère, J. M.; Adolph, H. W. *FEBS Lett.* **1998**, *438*, 137−140.
(11) Kaminskaia, N. V.; Spingler, B.; Lippard, S. J. *J. Am. Chem. Soc.* **2000**, *122*, 6411−6422.
(12) Fast, W.; Wang, Z.; Benkovic, S. J. *Biochemistry* **2001**, *40*, 1640−1650.

10.1021/ja0113246 CCC: $20.00
Published on Web 09/14/2001

The structure of the *B. cereus* enzyme has been determined by X-ray crystallography at 1.85−2.5 Å resolution by using crystals grown with different zinc(II) concentrations (100−500 μM) at slightly acid pH 5.2−5.6.[13−15] In these structures, the essential zinc ion (Zn1) is tetrahedrally coordinated by three histidine residues (His86, His88, His149) and a water molecule (Wat1). The location of Wat1 varies significantly having Zn1−Wat1 distances of 2.3−3.3 Å in the different structures reported to date. Depending on the enzyme:zinc(II) molar ratio, a second zinc ion (Zn2) can be coordinated by the carboxylate group of an aspartate (Asp90), the methylthiolate group of a cysteine (Cys168), the imidazole ring of a histidine (His210), the Zn1-bound Wat1 molecule, and a second water molecule, Wat2. According to rigid docking analyses, the *B. cereus* enzyme has an accessible active site that can accommodate β-lactam substrates with very different side chains attached to the β-lactam nucleus.[15] Substrates have been located such that the β-lactam carboxylate and carbonyl point toward the conserved residues Lys171 and Asn180, respectively. In these models, the orientation of the β-lactam substrate with respect to Wat1 appears favorable for nucleophilic attack to occur. In many zinc-enzymes, the deprotonated form of zinc-bound water is the most favorable form at physiological pH (p$K_a \sim 7$), where it has an enhanced nucleophilic ability.[16] Recent quantum chemical calculations on cluster models of zinc enzymes have also suggested that the presence of a carboxylate group close to the zinc ion would deprotonate the zinc-bound water molecule.[17] Thus, it is commonly thought that the Zn1-bound water is present in its unprotonated form in the *B. cereus* active site and therefore would readily attack the β-lactam carbonyl.

The kinetics of the catalytic mechanism of the *B. cereus* enzyme has been investigated by using various β-lactam substrates (benzylpenicillin, cephalorodine, nitrocefin).[18,19] In cryoenzymology experiments, it has been observed that the pre-steady kinetics requires a branched catalytic pathway for the Zn(II), Mn(II), and Co(II) forms of the *B. cereus* enzyme. According to low-temperature acid quench experiments, the branched pathways comprise conformationally distinct noncovalent Michaelis complexes. The authors concluded that this may be a consequence of fluctuations of the protein.[18] Concerning the pH rate dependence of the catalytic mechanism, the plot of k_{cat}/K_m versus pH showed characteristic bell-shaped curves.[19] However, the slope of the acidic part of the curve was close to 2.0 instead of the usual 1.0, that is, the enzymatic efficiency is suppressed at lower pH because of *two* protonation processes. The corresponding rate controlling ionization constants, p$K_{a,1}$ = p$K_{a,2}$, and p$K_{a,3}$ were centered on values of 5.60 ± 0.20 and 9.50 ± 0.20, respectively. Although the assignment of p$K_{a,3}$ has not been definitively made, it has been proposed that the existence of a Zn−OH···O−CO−Asp90 interaction can account for p$K_{a,1}$ and p$K_{a,2}$.[19] In addition, it has been observed that the primary kinetic solvent isotope effect on k_{cat} has a value of ∼1.5, suggesting that proton motion is only moderate in the rate-determining transition state.

Scheme 1

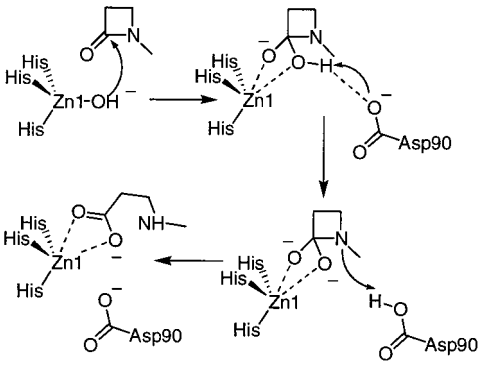

Scheme 2

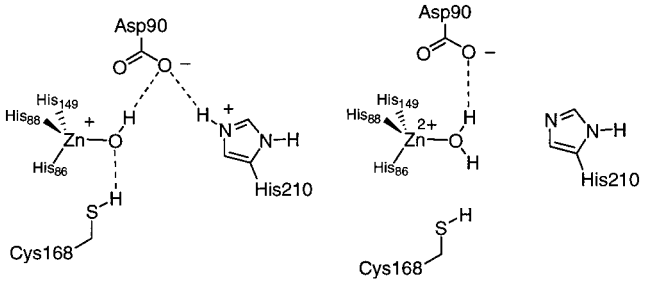

ZnOH **$ZnOH_2$**

On the basis of the kinetic and structural observations, it has been proposed that a Zn1-bound hydroxide nucleophile attacks the β-lactam carbonyl carbon forming a tetrahedral intermediate in which the β-lactam ring is not cleaved.[19] The interaction between the Zn1 cation and the negative charge developed on the β-lactam oxygen atom stabilizes this hypothetical intermediate (see Scheme 1). Subsequently, the Asp residue, initially hydrogen bonded to the Wat1 molecule, would accept a proton from the hydroxyl moiety in the intermediate and, as the β-lactam C−N bond fission proceeds, protonate the leaving amino group. It has also been proposed that the rate-determining step corresponds to one of the two proton-transfer processes. This mechanistic proposal assumes the participation of a dianionic species to explain the second-order dependence of reactivity on the H^+ concentration at low pH although there is no direct evidence to support the existence of intermediate species in the catalytic cycle of the monozinc enzymes. We also note that this mechanism has no significant role for the His210 and Cys168 residues which are known to be crucial for catalysis according to mutagenesis experiments.[20,21]

Very recently, we have studied the structure and dynamics of the *B. cereus* enzyme in its mononuclear form by using Molecular Dynamics (MD) simulations.[22] We considered two different protonation states of the active site (**ZnOH** and **$ZnOH_2$** in Scheme 2) which are formally interconnected via a proton transfer from a doubly protonated His210 residue to a zinc-bound hydroxide moiety. In these simulations, a bifurcated salt bridge between the carboxylate group of Asp90 and the zinc-bound hydroxide and the doubly protonated His210 residue was important for the structure of the **ZnOH** model. This is consistent with the characteristics ascribed to Asp90 and His210

(13) Carfi, A.; Pares, S.; Duée, E.; Galleni, M.; Duez, C.; Frère, J. M.; Dideberg, O. *EMBO J.* **1995**, *14*, 4914−4921.
(14) Carfi, A.; Duée, E.; Galleni, M.; Frère, J. M.; Dideberg, O. *Acta Crystallogr. D* **1998**, *54*, 313−323.
(15) Fabiane, S. M.; Sohi, M. K.; Wan, T.; Payne, D. J.; Bateson, J. H.; Mitchell, T.; Sutton, B. J. *Biochemistry* **1998**, *37*, 12404−12411.
(16) Lipscomb, W. N.; Sträter, N. *Chem. Rev.* **1996**, *96*, 2375−2433.
(17) Deerfield, D. W.; Carter, C. W. J.; Pedersen, L. G. *Int. J. Quantum Chem.* **2001**, *83*, 150−165.
(18) Bicknell, R.; Waley, S. G. *Biochemistry* **1985**, *24*, 6876−6887.
(19) Bounaga, S.; Laws, A. P.; Galleni, M.; Page, M. I. *Biochem. J.* **1998**, *331*, 703−711.
(20) Hilliard, N. P.; Clark, S. D.; Shaw, R. W. *Fase B J.* **1994**, *8*, A1365−A1365.
(21) Chantalat, L.; Duée, E.; Galleni, M.; Frère, J. M.; Dideberg, O. *Protein Sci.* **2000**, *9*, 1402−1406.
(22) Suárez, D.; Merz, K. M., Jr. *J. Am. Chem. Soc.* **2001**, *123*, 3759−3770.

by mutagenesis experiments.[20,23] Similarly, we proposed that within the Zn−OH···Asp90···His210 hydrogen bonding network, the His210 residue might have a high pK_a value while the accompanying pK_a lowering in the Zn−OH···Asp90 moiety, which has two proton acceptor sites, would formally correspond to the zinc-bound water. The rest of the structural and dynamical properties of the **ZnOH** configuration give further support to this model as the kinetically active configuration of the mononuclear *B. cereus* system. For the second configuration studied, **$ZnOH_2$**, our analyses indicated that this configuration corresponds to an intermediate stage during the regeneration of the active site in the absence of substrate. Interestingly, we also observed that the actual energy difference between **ZnOH** and **$ZnOH_2$** is likely not to be large and, therefore, an equilibrium between the **ZnOH** and **$ZnOH_2$** configurations might be expected.

In this article, we present our results from MD simulations of the Michaelis complex of the *B. cereus* enzyme with benzylpenicillin, which is a typical representative of the substrate profile exhibited by *B. cereus*. The structural and dynamical effects induced by substrate-binding, the specific role of the conserved residues in promoting substrate binding, and the determination of near attack conformers[24] of the Michaelis complex are discussed based on the MD trajectories. Quantum Mechanical (QM) methods are subsequently applied to study the hydrolysis reaction of *N*-methylazetidinone catalyzed by a monozinc system consisting of the side chains of the histidine residues (His86, His88, His149) complexed with Zn−OH and the side chains of Asp90 and His210. To further asses the viability of the mechanistic route revealed by the model system, we built molecular mechanics (MM) models of the prereactive complex and the transition state configurations embedded within the *B. cereus* active site. To estimate their energies, we also performed linear-scaling semiempirical calculations coupled with a continuum solvent model to account for environmental effects. On the basis of the theoretical results, we reinterpret the experimental kinetic data of the *B. cereus* enzyme in terms of a single one-step mechanism for the hydrolysis of β-lactam substrates in which His210 acts as a proton donor.

Computational Methods

Parametrization of the Zinc Environment and Benzylpenicillin. As in our previous MD simulations of the free form of the *B. cereus* enzyme,[22] we adopted the bonded approach for the metal ion representation, which involves placing explicit bonds between the zinc cation and its surrounding environment.[25,26] To derive the corresponding force-field parameters which are not present in the standard AMBER database, we followed the procedure suggested by Fox et al.[27] to be consistent with the AMBER force field.[28] Further details of the zinc parametrization can be found elsewhere.[22]

Benzylpenicillin (BP) was fully optimized at the HF/6-31G* QM level of theory to compute the electrostatically derived atomic charges[29] using the RESP methodology.[30] Further structural data required to represent the equilibrium geometry of the bicyclic skeleton of benzylpenicillin (e.g., the bond distances and bond angles in the β-lactam ring) were extracted from the HF/6-31G* optimized structure. Most of the bond, angle, and dihedral parameters of BP were available in the AMBER force field. The missing parameters were assigned the values of similar types in the force field. The vdW parameters were taken from the closest existing AMBER atom types according to the electronic structure similarity. This BP parametrization was tested by minimizing in vacuo the geometry of BP, the resultant structure being quite similar to the HF/6-31G* one (the HF/6-31G* BP equilibrium geometry, the RESP charges, and atom types are given in the Supporting Information).

MD Simulations. The determination of an initial enzyme−ligand complex was necessary to obtain a starting configuration for the MD studies. We employed the algorithm developed for AutoDock,[31,32] which uses a Monte Carlo simulated annealing technique for configurational exploration of enzyme−ligand complexes with a rapid energy evaluation using grid-based molecular interaction potentials (built from van der Waals and electrostatic contributions). The BP substrate was docked in the static binding site of the *B. cereus* zinc-β-lactamase. During the docking process, the internal bonds of the BP side chains were allowed to rotate. The coordinates of the protein atoms were taken from the *B. cereus* 1.85 Å crystal structure of Carfi et al. (PDB ID code 1BME).[14] This high-resolution structure shows one fully and one partially occupied zinc site and for our purposes we deleted the second zinc ion and a carbonate anion from the coordinate file.

The most stable enzyme−substrate complex obtained in our automatic docking calculations was in good agreement with those reported in previous docking analyses[15] (e.g. the β-lactam carboxylate and carbonyl pointed toward the Lys171 ammonium and the Asn180 side chain, respectively). This enzyme−substrate complex, as well as the water molecules of the crystal structure, was surrounded by a periodic box of TIP3P water molecules which extended 10 Å from the protein and substrate atoms. This resulted in the enzyme−substrate system (3501 atoms) being solvated by 208 X-ray water molecules and 9476 additional water molecules. All of the ionizable residues were set to their pH 7 protonation states except His210, which was positively charged. A Cl^- counterion was placed 20 Å beyond the zinc atom to neutralize the +1 charge of the enzyme−substrate model with use of the LEaP software.[33] The parm96 version of the all-atom AMBER force field was used to represent the system.[28]

To remove bad contacts in the initial geometry, energy minimization was done by using a conjugate-gradient minimizer (2500 steps for the water molecules followed by 2500 steps for the whole system). MD simulations were carried out by using the SANDER program included in the version 5.0 of the AMBER package.[34] The time step was chosen to be 1.5 fs and the SHAKE algorithm[35] was used to constrain all bonds involving hydrogen atoms. A nonbond pairlist cutoff of 10.0 Å was used and the nonbonded pairlist was updated every 25 time steps.[36] The pressure (1 atm) and the temperature (300 K) of the system were controlled during the MD simulations by Berendsen's method[37] (a separate scaling factor for the solute and the solvent temperatures was used). Periodic boundary conditions were applied to simulate a continuous system.[36] To include the contributions of long-range interactions, the Particle−Mesh−Ewald (PME) method[38] was used with a grid size of 64 × 64 × 64 (grid spacing of ∼1 Å) combined with a

(23) Lim, H. M.; Iyer, R. K.; Pène, J. J. *Biochem. J.* **1991**, *276*, 401−404.
(24) Bruice, T. C.; Benkovic, S. *Biochemistry* **2000**, *38*, 6267−6274.
(25) Hoops, S. C.; Anderson, K. W.; Merz, K. M., Jr. *J. Am. Chem. Soc.* **1991**, *113*, 8262−8270.
(26) Ryde, U. *Proteins* **1995**, *21*, 40−56.
(27) Fox, T.; Kollman, P. A. *J. Phys. Chem. B* **1998**, *102*, 8070−8079.
(28) Cornell, W. D.; Cieplak, P.; Bayly, C. I.; Gould, I. R.; Merz, K. M., Jr.; Ferguson, D. M.; Spellmeyer, D. C.; Fox, T.; Caldwell, J. W.; Kollman, P. A. *J. Am. Chem. Soc.* **1995**, *117*, 5179−5197.
(29) Besler, B. H.; Merz, K. M., Jr.; Kollman, P. A. *J. Comput. Chem.* **1990**, *11*, 431−439.
(30) Bayly, C. A.; Cieplak, P.; Cornell, W. D.; Kollman, P. A. *J. Phys. Chem.* **1993**, *97*, 10269−10280.
(31) Morris, G. M.; Goodsell, D. S.; Halliday, R. S.; Huey, R.; Hart, W. E.; Belew, R. K.; Olson, A. J. *J. Comput. Chem.* **1998**, *19*, 1639−1662.
(32) Goodsell, D. S.; Olson, A. J. *Proteins: Struct. Func. Genet.* **1990**, *8*, 195−202.
(33) Schafmeister, C.; Ross, W. S.; Romanovski, V. *LEap*, 1.0 ed.; University of California: San Francisco, 1995.
(34) Case, D. A.; Pearlman, D. A.; Caldwell, J. W.; Cheatham, T. E., II; Ross, W. S.; Simmerling, C. L.; Darden, T. A.; Merz, K. M., Jr.; Stanton, R. V.; Cheng, A. L.; Vincent, J. J.; Crowley, M.; Ferguson, D. M.; Radmer, R. J.; Seibel, G. L.; Singh, U. C.; K., W. P.; Kollman, P. A. *AMBER*, 5.0 ed.; University of California: San Francisco., 1997.
(35) van Gunsteren, W. F.; Berendsen, H. J. C. *Mol. Phys.* **1977**, *34*, 1311.
(36) Allen, M. P.; Tildesley, D. J. *Computer Simulation of Liquids*; Clarendon Press: Oxford, 1987.
(37) Berendsen, H. J. C.; Potsma, J. P. M.; van Gunsteren, W. F.; DiNola, A. D.; Haak, J. R. *J. Chem. Phys.* **1984**, *81*, 3684−3690.
(38) Essman, V.; Perera, L.; Berkowitz, M. L.; Darden, T.; Lee, H.; Pedersen, L. G. *J. Chem. Phys.* **1995**, *103*, 8577−8593.

Scheme 3

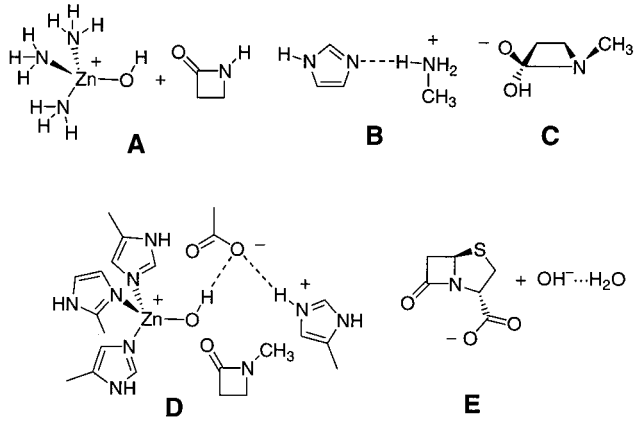

fourth-order *B*-spline interpolation to compute the potential and forces between grid points. The estimated root-mean-squared deviation of the PME force errors[39] was lower than 10^{-4} during the simulations.

An equilibration period of 200 ps resulted in a stable trajectory (as evidenced by convergence of the dimensions of the simulation box and the evolution of the total energy of the system). Subsequently, a 1 ns trajectory was computed and coordinates were saved for analyses every 50 time steps. All of the MD results were analyzed by using the CARNAL module of AMBER 5.0 and some specific trajectory analysis software developed locally.

QM Calculations. To calibrate the methodology to be used in the QM study of the enzymatic mechanism, we investigated, at high levels of theory, the Potential Energy Surface (PES) of small systems relevant to the basic chemical events which occur during the enzymatic hydrolysis of β-lactams (see Scheme 3). Thus, we considered the system **A** as a model that characterizes the nucleophilic attack of the zinc-bound hydroxide on the β-lactam carbonyl. The energetic cost for proton transfer and for the rupture of the β-lactam ring was analyzed via model systems **B** and **C**, respectively. For the systems **A**, **B**, and **C**, all the optimizations were done in the gas phase with no constraints at the HF/6-31G*, B3LYP/6-31G*, and MP2/6-31G* levels of theory.[40,41] The critical structures were further characterized by analytical computation of harmonic frequencies at the HF/6-31G* and B3LYP/6-31G* levels. Electronic energies for the MP2/6-31G* optimized structures were recomputed for the nonmetallic model systems **B** and **C** by using the G2(MP2,SVP) scheme.[42] For the model system **A**, electronic energies were refined by means of single-point MP4/6-31G* and MP2/6-311+G(2d,2p) calculations.

As a more realistic model for the enzymatic process, we considered the cluster model **D** shown in Scheme 3. In this model system, the C atoms in the methyl groups were held fixed at their X-ray equilibrium position during optimization of critical structures at the HF/3-21G*, HF/6-31G*, and B3LYP/6-31G* levels of theory. The large size of this system (72 atoms, around 600 basis functions) prevented us from carrying out frequency calculations with the 6-31G* basis set. The corresponding analytical Hessians were, therefore, calculated at the HF/3-21G* level. Thermodynamic data (298 K, 1 bar) were computed by using the HF/3-21G* frequencies within the ideal gas, rigid rotor, and harmonic oscillator approximations (the contribution of the residual gradient due to the constraints was removed from the Hessian matrix by using a simple projection operator[43]). The nature of the Zn−ligand and reactive bonds was further analyzed by calculating the corresponding Bond Critical Point (BCP) properties in the B3LYP/6-31G* charge density $\rho(\mathbf{r}_c)$[44] (some BCP properties are reported as Supporting Information). To roughly estimate condensed-phase effects, we computed solvation free energies in aqueous solution by means of single-point B3LYP/6-31G* Self-Consistent Reaction Field Poisson−Boltzmann (SCRF-PB) calculations, where the solute is represented by a set of atomic charges and the solvent as a layer of charges at the solute molecular surface.[45]

Model **E** in Scheme 3 represents the alkaline hydrolysis of 3α-carboxypenam, a penicillin model compound, reacting with a hydroxide anion solvated by a explicit water molecule. For this reference reaction, we only located the transition structure for the rate-determining nucleophilic attack at the B3LYP/6-31+G* level (i.e., diffuse basis functions were included to treat this dianionic system). Thermal corrections were included at the HF/3-21G* level while solvent effects were considered by single-point B3LYP/6-31+G* SCRF-PB calculations.

All the ab initio and DFT QM calculations in the gas phase were done with use of the Gaussian98 suite of programs.[46] Solvation energies were computed with use of the SCRF-PB module of JAGUAR.[47] Atomic charges were also computed for all the structures according to the Natural Population Analysis scheme.[48]

Linear Scaling Semiempirical Calculations. Single-point PM3[49,50] calculations were performed on two models of the *B. cereus* enzyme complexed with benzylpenicillin which represent a prereactive configuration and a transition state configuration, respectively. These calculations were done by using the Divide and Conquer (D&C) approach.[51,52] Explicit solvent molecules were not considered. Incorporation of solvent effects was accomplished by means of single-point semiempirical calculations, using the D&C algorithm merged with the Poisson−Boltzmann (PB) equation.[53] The resultant solvation energies incorporate long-range solute−solvent interactions and the statistical weight of different solvent configurations. The DivCon99 program[52] was employed to perform the D&C and D&C-PB PM3 calculations using the dual buffer layer scheme (inner buffer layer of 5.0 Å and an outer buffer layer of 2.0 Å) with one protein residue per core. This D&C *subsetting* with a total buffer region of 7.0 Å gives generally accurate energies.[54] A cutoff of 9.0 Å was used for the off-diagonal elements of the Fock, 1-electron, and density matrices. The D&C-PB calculations were carried out by using the computational protocol described in detail elsewhere.[53]

In this work, we employed a new PM3 parametrization for zinc, which has been obtained by using a genetic algorithm in our laboratory. The parametrization reference set, which maintains the thermochemical data used to obtain the original PM3 parameters, was augmented with

(39) Petersen, H. G. *J. Chem. Phys.* **1995**, *103*, 3668−3679.
(40) Hehre, W. J.; Radom, L.; Schleyer, P. v. R.; Pople, J. A. *Ab Initio Molecular Orbital Theory*; John Wiley & Sons: New York, 1986.
(41) Becke, A. D. *Exchange-Correlation Approximation in Density-Functional Theory*; Yarkony, D. R., Ed.; World Scientific: Singapore, 1995.
(42) Curtiss, L. A.; Redfern, P. C.; Smith, B. J.; Radom, L. *J. Chem. Phys.* **1996**, *104*, 5148−5152.
(43) Peng, Z.; Merz, K. M., Jr. *J. Am. Chem. Soc.* **1993**, *115*, 9640−9647.
(44) Bader, R. F. W. *Atoms in Molecules. A Quantum Theory*; Clarendon: Oxford, 1990.
(45) Tannor, D. J.; Marten, B.; Murphy, R.; Friesner, R. A.; Sitkoff, D.; Nicholls, A.; Ringnalda, M.; Goddard, W. A., III; Honig, B. *J. Am. Chem. Soc.* **1994**, *116*, 11875−11882.
(46) Frisch, M. J.; Trucks, G. W.; Schlegel, H. B.; Scuseria, G. E.; Robb, M. A.; Cheeseman, J. R.; Zakrzewski, V. G.; Montgomery, J. A.; Stratmann, R. E., Jr.; Burant, J. C.; Dapprich, S.; Millam, J. M.; Daniels, A. D.; Kudin, K. N.; Strain, M. C.; Farkas, O.; Tomasi, J.; Barone, V.; Cossi, M.; Cammi, R.; Mennucci, B.; Pomelli, C.; Adamo, C.; Clifford, S.; Ochterski, J.; Petersson, G. A.; Ayala, P. Y.; Cui, Q.; Morokuma, K.; Malick, D. K.; Rabuck, A. D.; Raghavachari, K.; Foresman, J. B.; Cioslowski, J.; Ortiz, J. V.; Stefanov, B. B.; Liu, G.; Liashenko, A.; Piskorz, P.; Komaromi, I.; Gomperts, R.; Martin, R. L.; Fox, D. J.; Keith, T.; Al-Laham, M. A.; Peng, C. Y.; Nanayakkara, A.; Gonzalez, C.; Challacombe, M.; Gill, P. M. W.; Johnson, B.; Chen, W.; Wong, M. W.; Andres, J. L.; Gonzalez, C.; Head-Gordon, M.; Replogle, E. S.; Pople, J. A. *Gaussian 98*, A.6 ed.; Gaussian: Pittsburgh, PA, 1998.
(47) *JAGUAR*, 3.5 ed.; Schrödinger, Inc.: Portland, OR, 1998.
(48) Reed, A. E.; Weinstock, R. B.; Weinhold, F. *J. Chem. Phys.* **1985**, *83*, 735−746.
(49) Stewart, J. J. P. *J. Comput. Chem.* **1989**, *10*, 221−264.
(50) Stewart, J. J. P. *J. Comput. Chem.* **1991**, *12*, 320−341.
(51) Yang, W.; Lee, T.-S. *J. Chem. Phys.* **1995**, *103*, 5674−5678.
(52) Dixon, S. L.; van der Vaart, A.; Gogonea, V.; Vincent, J. J.; Brothers, E. N.; Suárez, D.; Westerhoff, L. M.; Merz, K. M. J. *DIVCON99*; The Pennsylvania State University, 1999.
(53) Gogonea, V.; Merz, K. M., Jr. *J. Phys. Chem. A* **1999**, *103*, 5171−5178.
(54) van der Vaart, A.; Suárez, D.; Merz, K. M., Jr. *J. Chem. Phys.* **2000**, *113*, 10512−10523.

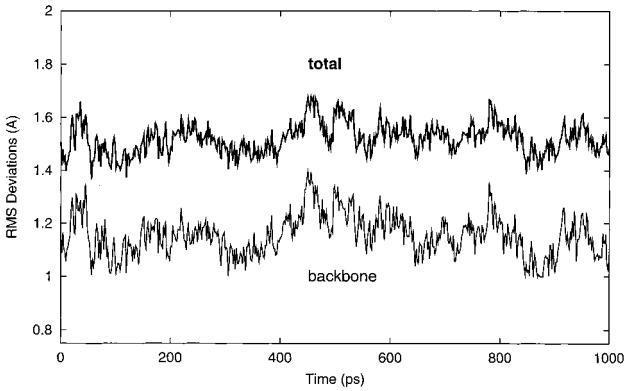

Figure 1. Root-mean-squared deviation between the instantaneous computed structures and the crystal structure for the *B. cereus* enzyme as a function of time in the **ZnOH-BP** simulation.

structural and energetic data obtained from ab initio model systems of zinc-enzymes (further details will be published elsewhere).[55]

Results

MD Simulation of the Michaelis Complex between Benzylpenicillin and the *B. Cereus* Zinc-β-lactamase. We simulated the *B. cereus* enzyme complexed with benzylpenicillin (**ZnOH-BP** model). The active site region represented by the **ZnOH** configuration has a zinc-bound hydroxide moiety while the nearby His210 residue is protonated.[22] The time evolution of the root-mean-squared deviation (RMSD) of the *B. cereus* zinc-β-lactamase protein relative to the crystal structure is shown in Figure 1. The protein atoms of the **ZnOH-BP** model did not significantly deviate from the crystal structure and had average RMSD values (1.52 ± 0.06 total, 1.15 ± 0.08 Å backbone) which are similar to those observed in other protein simulations. Note that the fluctuations of the RMSD values around their mean values were also moderate. We conclude that the structural changes were quite small over time, suggesting that the **ZnOH-BP** model evolved in an equilibrium state with respect to the RMS deviations during the analyzed trajectory.

The RMS flexibility (RMSF) was calculated by comparing the instantaneous protein structure to the average one. The calculated RMSF value for the entire protein in the **ZnOH-BP** model (0.87 ± 0.07 Å) was similar to that previously obtained for the free enzyme (0.92 ± 0.07 Å). We also compared the per residue RMSF values with those estimated by experimental *B*-factors (see Figure 2). In general, regions that had greater flexibility in the crystal structure also had greater flexibility in the MD simulation although the magnitude of the calculated fluctuations in solution tended to be lower than what was observed in the solid state (also see Supporting Information).

Structure of the Active Site. A typical snapshot of the active site region and a schematic representation of the most important interresidue and enzyme−substrate contacts observed during the **ZnOH-BP** simulation are shown in Figure 3. The mean values for some of the more significant interatomic distances between the zinc ion and the nearby residues are collected in Table 1 while the average distance between heavy atoms and lifetimes for selected H-bond contacts are summarized in Table 2.

During the MD simulation of the Michaelis complex (**ZnOH-BP**), the overall architecture of the active site is very similar to that of the free enzyme (**ZnOH**).[22] Thus, the carboxylate group of Asp90 has a bifurcated salt bridge with the Zn-OH moiety and with the His210 Nε2-Hε2 bond throughout the **ZnOH-BP** simulation (the Oδ2@Asp90···O−Zn and Oδ2@Asp90···Nε2@His210 average distances are 2.99 and 2.75 Å, respectively). The imidazole ring of His210 is close to the zinc bound hydroxide nucleophile because of a weak Nε2−Hε2···OH−Zn contact via a single H-bond that occurs 50.0% of the time (average Nε2···O distance of 3.69 Å). In addition, the thiol group of Cys168 further stabilizes the nucleophile via a Sγ−Hγ···O hydrogen bond (see Table 2). Note that these and other contacts have been thoroughly discussed.[22] On the other hand, some changes can be identified with respect to the unbound **ZnOH** model. For example, the salt bridge between Arg91 and Asp56, which is thought to be important for the architecture of the active site in the native form of the enzyme,[14] is altered upon substrate binding. In the **ZnOH-BP** model, the guanidinium group of Arg91 also interacts with the O and Oδ2 atoms of Asp90 while the carboxylate of Asp56 interacts with the backbone NH of Thr85. Asp56 is a conserved residue in the metallo-β-lactamases and it is the only residue with a φ angle outside the allowed range.[14] Moreover, the unusual φ angle for Asp56 is slightly larger in the **ZnOH-BP** simulation (63 ± 11°) than in the **ZnOH** one (58 ± 10°).

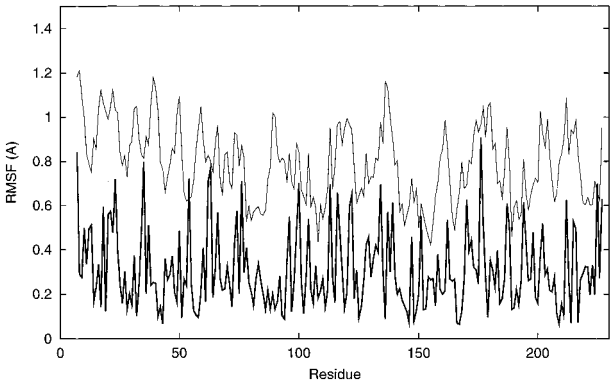

Figure 2. Plot of the average root-mean-squared flexibility per residue in the **ZnOH-BP** model. The thin line corresponds to the flexibility per residue in the solid state obtained from the *B* factors.

Table 1. Summary of Some Significant Interatomic Distances (Å) in the Active Site of the *B. cereus* Metallo-β-lactamase

distance	**ZnOH-BP**	**ZnOH**
Zn−O	1.85 ± 0.04	1.86 ± 0.04
Zn···Oδ1@Asp90	4.68 ± 0.31	4.56 ± 0.41
Zn···Oδ2@Asp90	3.87 ± 0.23	4.41 ± 0.38
Zn···Nε2@His210	5.78 ± 0.36	5.81 ± 0.35
Zn···Sγ@Cys168	4.58 ± 0.24	4.45 ± 0.17
Nε2@His210···Oδ2@Asp90	2.76 ± 0.13	2.73 ± 0.09

In the **ZnOH-BP** model, the pair distribution function *g*(r) for the zinc ion to the oxygen atoms in the surrounding water reveals the presence of approximately three solvation layers centered at distances of 4, 5, and 6 Å, respectively (see Figure 4). The integrated value of the first peak (1.00) corresponds to the presence of a "deep" water molecule in the vicinity of the zinc-bound hydroxide moiety, the Cys168 thiol group, and the BP carboxylate group. The second peak with an integrated value of 1.92 represents the solvation of the zinc ligands (each of the imidazole NH groups in His86, His88, and His149 interacts with a close water molecule on average). The solvation of the catalytically important residues (Asp90, His210, and Cys168) was found to be poor in the unbound **ZnOH** model,[22] and this is further reduced by the presence of the β-lactam substrate.

Enzyme−Substrate Binding Determinants. The majority of zinc-β-lactamases show a broad spectrum affinity for β-lactam substrates with very different side chains attached to

(55) Brothers, E. N.; Suárez, D.; Deerfield, D. W.; Merz, K. M. Manuscript in preparation, 2001.

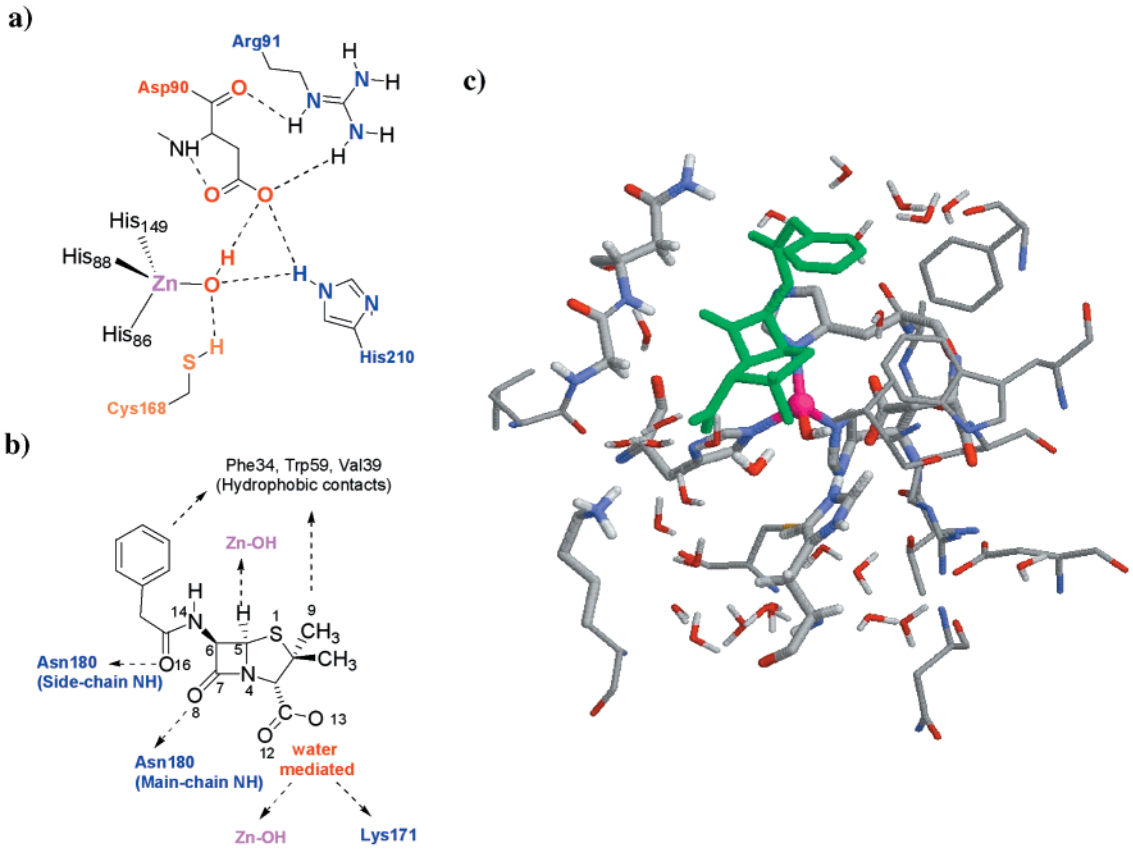

Figure 3. (a) Schematic representation of the most important interactions characterizing the active site of the **ZnOH-BP** model. (b) Enzyme−substrate binding determinants between benzylpenicillin and the *B. cereus* enzyme. Numbering of the benzylpenicillin atoms. (c) Snapshot of the **ZnOH-BP** active site.

Table 2. Summary of the Average Distances between Heavy Atoms (Å) and Percent Occurrence Data of Important Hydrogen Bonding Interactions within the Active Site of the *B. cereus* Metallo-β-lactamase Complexed with Benzylpenicillin

H-bond	X···Y	%	H-bond	X···Y	%
Asp90−Oδ2···HO−Zn	2.99 ± 0.21	100.0	Asp90−Oδ1···H−Nη1−Arg91	2.94 ± 0.23	99.0
Asp90−Oδ1···HO−Zn	3.23 ± 0.26	99.2	Asp56−Oδ1···H−N−Thr85	2.81 ± 0.09	100.0
ZnO···H−Nϵ2−His210	3.69 ± 0.28	50.0	Asp56−Oδ1···H−Oγ−Thr85	2.74 ± 0.15	100.0
ZnO···H−Sγ−Cys168	3.33 ± 0.20	85.1	BP−O16···H−Nδ2−Asn180	3.03 ± 0.28	62.9
Asp90−Oδ2···H−Nϵ2−His210	2.75 ± 0.12	98.6	BP−O8···H−N−Asn180	3.01 ± 0.22	80.2
Thr85−Oγ···H−Nδ1−His86	3.61 ± 0.23	82.5	BP−S1···H−N14−BP	3.02 ± 0.10	75.2
Asp90−O···H−Nϵ−Arg91	3.14 ± 0.21	68.2	Zn−O···H−C5−BP	3.36 ± 0.10	37.0
Asp90−Oδ2···H−Nϵ-Arg91	2.91 ± 0.20	97.0			

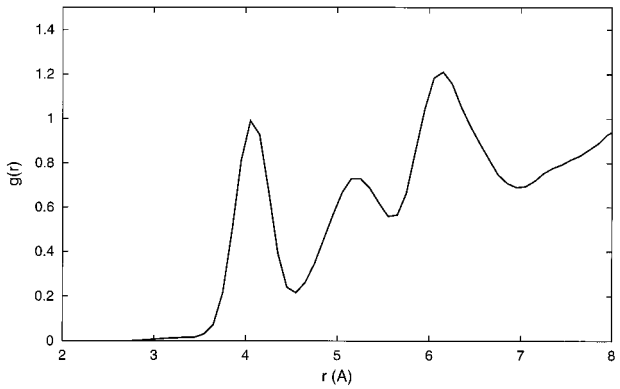

Figure 4. Atomic Radial distribution function g(r) for the zinc ion to the oxygens in the surrounding water molecules.

the β-lactam nucleus. During the **ZnOH-BP** simulation, binding of the antibiotic to the *B. cereus* enzyme occurs through the combination of hydrophobic forces and direct or water-mediated H-bond contacts with specific protein residues. These interactions can provide major substrate-binding determinants for almost all β-lactams.

In agreement with previous proposals,[15] we found that the conserved residues Asn180 and Lys171 play a central role in substrate binding. For example, the backbone N atom of Asn180 interacts with the β-lactam carbonyl group through a long-lived H-bond contact with an average N@Asn180···O8@BP distance of 3.01 ± 0.22 Å (% occurrence = 80.2%; see the numbering of the β-lactam atom positions in Figure 3b). In addition, the Asn180 side chain hydrogen bonds with the carbonyl group of the β-lactam 6-acylamino side chain (Nδ2−Hδ2···O16; % occurrence = 62.9%). The β-lactam carboxylate group was oriented toward the Lys171 ammonium group throughout the MD simulation; however, the interaction between these charged groups was mediated by water bridges consisting of one or two water molecules (i.e., O···$(H_2O)_n$···H−Nζ structures).[56] Thus, the O12 and O13 atoms of BP have an one-water molecule bridge in 83.4% and 68.5% of the analyzed trajectory, while

(56) Toba, S.; Colombo, G.; Merz, K. M., Jr. *J. Am. Chem. Soc.* **1999**, *121*, 2290−2302.

Table 3. Summary of the Significant Distances (Å) and Angles between the Hydrophobic Residues Phe34, Val39, and Trp59

distances		angles	
Ring@Phe34···Ring@Trp59	5.70 ± 0.45	Ring@Phe34···Cβ@Val39···Ring@Trp59	54.1 ± 6.09
Cβ@Val39···Ring@Phe34	6.79 ± 0.51	Ring@BP···Ring@Phe34	99.1 ± 17.8
Cβ@Val39···Ring@Trp59	5.51 ± 0.40	Ring@Phe34···Ring@Trp59	64.3 ± 12.4
Nδ1@His210···Cη2@Trp59	4.72 ± 0.49	Ring@His210···Ring@Trp59	68.7 ± 9.70
Ring@BP···Ring@Phe34	6.11 ± 0.85		
C9@BP···Cβ@Val39	6.27 ± 0.88		

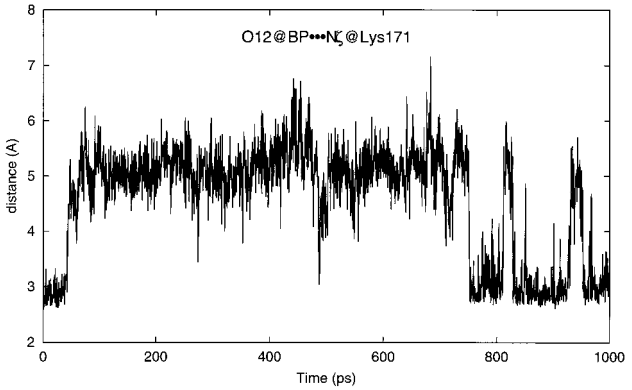

Figure 5. Separation (Å) between the O12 atom of the BP carboxylate and the Nζ atom of the positively charged Lys171 during the simulation.

linear bridges consisting of 2 water molecules were less frequent (∼30%). Nevertheless, a direct salt bridge interaction between the BP carboxylate group and Lys171 was observed in ∼20% of the analyzed frames. Figure 5 displays a histogram of the distances between the Nζ@Lys171 atom and the carboxylate O12 atom reflecting the flexibility of this salt bridge interaction.

It is interesting to note that, during 90.5% of the simulation time, the "deep" water molecule links the Zn−OH moiety and the BP carboxylate through two O−H···O hydrogen bonds with average distances of 2.74 Å (Zn−O···O) and 2.76 Å (O···O−C). This double-donor one-water molecule bridge (Zn−O···H−O−H···O−CO) had lifetimes ranging from 13 to 200 ps. Thus, we see that this "deep" water molecule is another significant binding determinant that may be important in properly orienting the substrate for catalysis. Although an active catalytic role for this water molecule could be possible, we also note that it must be displaced prior to nucleophilic attack by the zinc-bound hydroxide ion.

One of the important features observed in the **ZnOH** simulation of the free form of the enzyme[22] was the presence of a stable hydrophobic cluster of residues adjacent to the zinc cation (Val39, Trp59, Phe34). We predicted that the hydrophobic side chains of these residues could bind the lipophilic regions of the substrate. This is confirmed by the MD analysis of the **ZnOH-BP** enzyme−substrate complex, which shows the BP phenyl group and the Phe34 side chain in a T-shaped orientation (a favorable disposition normally observed in $\pi-\pi$ interactions[57]). These interactions are geometrically characterized in Table 3 on the basis of distances and angles involving the center of mass of the Trp59 and Phe34 side chains, the center of mass of the BP phenyl group, the position of the C2-methyl groups of BP, and the Cβ@Val39 atom. For example, the Phe34···BP $\pi-\pi$ interaction results in a distance between the phenyl centers of mass of 6.11 Å and an average angle between the phenyl planes of 99.1°. The relative position of one of the C2-methyl groups and the Cβ atom of Val39 is 6.27 Å. Clearly, the stability of this hydrophobic clustering could be important for both promoting substrate binding and providing a relatively low polarity environment in the catalytic site. We also expect that the substrate specificity shown by the *B. cereus* enzyme could be partly modulated by interactions of the β-lactam substituents with this hydrophobic group of residues.

In our simulations, the β-lactam substrate also has a direct interaction with the zinc-bound nucleophile via a C−H···O contact[58,59] between the β-lactam C5 atom and the O atom of the Zn−OH moiety. The mean C5···O distance and C5−H···O angle are 3.68 ± 0.37 Å and 144.2 ± 12°. By applying the typical geometrical criteria for H-bond interactions (e.g., X···Y distance <3.5 Å), a short C−H···O interaction is present in 37.0% of the analyzed frames with an average distance of 3.36 ± 0.10 Å, suggesting that this contact may be relevant for substrate-binding and catalysis. In fact, a previous quantum chemical study on the alkaline hydrolysis of a β-lactam model compound[60] has shown that the transition state has similar C−H···O interactions with the C6 and C5 atoms of β-lactams. The distance between the zinc-bound nucleophilic oxygen and the carbonyl carbon of the β-lactam has a mean distance of 4.89 ± 0.47 Å.

Near Attack Conformers of the Michaelis Complex. We further analyzed the structure of the **ZnOH-BP** model by characterizing the population of enzyme−substrate complexes, which have close C7@BP···O−Zn distances between the β-lactam and the nucleophile. By assuming that a C7···O−Zn distance below 4.0 Å would be indicative of a near attack conformation (NAC),[24] we found that 1.7% of the observed configurations satisfied this criteria. Many more structures were very close to the 4.0 Å threshold: for example, 7.1% of the sampled structures had a C7···O−Zn contact below 4.25 Å. Thus, our simulations confirm that the **ZnOH** configuration of the *B. cereus* enzyme results in an enzyme−substrate complex that evolves dynamically passing through configurations poised for nucleophilic attack by the zinc-bound hydroxide.

We can estimate the expense of formation for the NAC conformations from the simulations using eq 1, where R is the

$$\Delta F = -RT \ln P \qquad (1)$$

gas constant, T is the temperature, ΔF is the free energy, and P is the probability of NAC formation. Using this approximation we estimate that NAC formation costs about 2.4 kcal/mol to form the sub-4.0 Å NAC conformers, while the sub-4.25 Å NACs cost ∼1.6 kcal/mol to form.

For the NAC complexes with C7···O−Zn < 4.0 Å, the average C7···O−Zn distance is 3.87 Å while the C7···O−Zn and O···C7═O8 angles have average values of 128° and 90°, respectively. Interestingly, the Zn−OH group is desolvated in the NAC structures, that is, the *deep* water molecule is shifted toward the β-lactam carboxylate group. Although catalytic zinc-

(57) Hobza, P.; Selzle, H. L.; Schalg, E. W. *J. Phys. Chem.* **1996**, *100*, 18790−18794.

(58) Desiraju, G. R. *Acc. Chem. Res.* **1991**, *24*, 290−296.

(59) Vargas, R.; Garza, J.; Dixon, D. A.; Hay, B. P. *J. Am. Chem. Soc.* **2000**, *122*, 4750−4755.

(60) Pitarch, J.; Ruiz-López, M. F.; Silla, E.; Pascual-Ahuir, J. L.; Tuñón, I. *J. Am. Chem. Soc.* **1998**, *120*, 2146−2155.

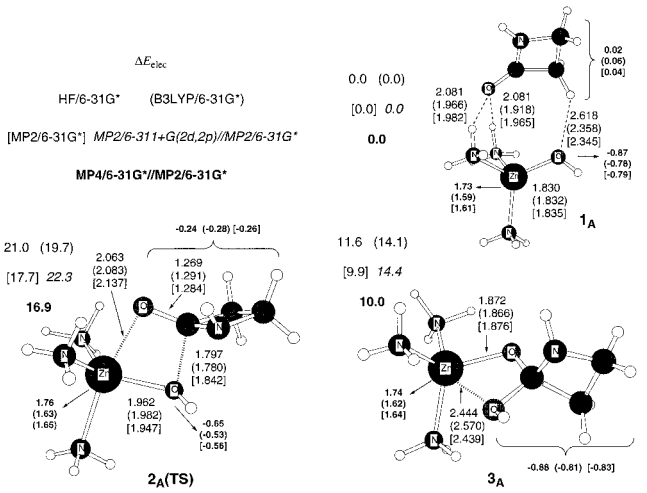

Figure 6. Optimized structures involved in the addition of the zinc-bound hydroxide in the $[Zn(NH_3)_3(OH)]^+$ complex to 2-azetidinone. Some significant distances (Å) and NPA charges are given at the HF/6-31G*, (B3LYP/6-31G*), and [MP2/6-31G*] levels of theory. Relative energies (kcal/mol) at different levels of theory are also indicated.

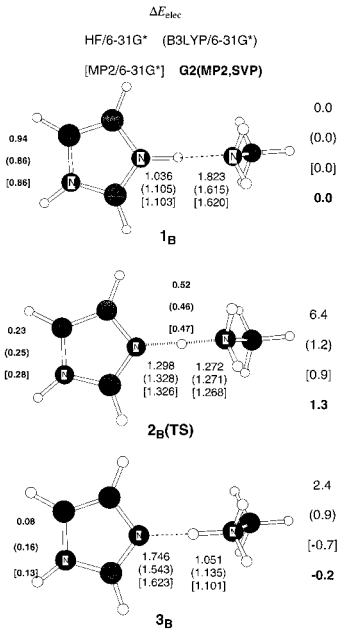

Figure 7. Optimized structures involved in the proton transfer between imidazole and methylammonium. Some significant distances (Å) and NPA charges are given at the HF/6-31G*, (B3LYP/6-31G*), and [MP2/6-31G*] levels of theory. Relative energies (kcal/mol) at different levels of theory are also indicated.

(II) ions are normally thought to polarize carbonyl substrates,[61] such an interaction is not present in the NAC complexes for the **ZnOH-BP** *B. cereus* model where the average Zn···O8@BP distance is 4.77 ± 0.34 Å. Interestingly, the carbonyl group of the β-lactam has weak C−H···O contacts with the Cϵ1 atoms of the zinc-ligands His88 and His149 in ∼40% of the NAC complexes (both Cϵ1@His···O8@BP distances are ∼3.7 Å). On the other hand, 10% of the NAC structures (0.2% of the simulation time) have both Zn−O···C7 and Nϵ2@His210··· N4@BP contacts of ∼3.8 Å. This means that the bifucarted H-bond of the Oδ2@Asp90 atom with the His210 Nϵ2−Hϵ2 bond and the Zn−OH group can be destabilized such that the nucleophilic attack of the Zn−OH group could simultaneously favor the reorientation of the His210 side chain to hydrogen bond with the endocyclic N atom of the β-lactam. In this case, the proton transfer from His210 to the leaving N atom could induce the cleavage of the β-lactam ring required to complete the hydrolysis reaction. These results clearly suggest that, for the *B. cereus* enzyme, the nucleophilic attack of the zinc-bound hydroxide group is accompanied by proton transfer from His210.

QM Studies of the Reaction Mechanism

Relative Performance of QM Levels of Theory. To further investigate the reactivity of the **ZnOH-BP** configuration, we carried out a computational study of the hydrolysis of a small β-lactam (*N*-methyl-azetidinone) catalyzed by a cluster model of the *B. cereus* active site (model **D** in Scheme 3). We employed QM methodologies (HF/6-31G* and B3LYP/6-31G*) to characterize a reaction pathway in which the positively charged His210 plays an active role as a proton donor. However, the degree of complexity of the reaction process and the size of this enzymatic model (72 atoms) prompted us to initially examine the relative performance of the HF/6-31G* and B3LYP/6-31G* levels of theory as applied to smaller systems relevant to catalysis. Thus, the geometries and charge distribution of the model systems **A**−**C** shown in Figures 6−8 were determined at the HF/6-31G*, MP2/6-31G*, and B3LYP/6-31G* levels.

Figure 6 shows the critical structures involved in the nucleophilic addition of the zinc-bound hydroxide in the $[Zn(NH_3)(OH)]^+$ model complex to the simplest β-lactam model (2-azetidinone). In the prereactive complex (**1$_A$** in Figure 6), the β-lactam carbonyl group is bound to two ammonia ligands through H-bond interactions with distances of ∼2.0 Å, the zinc-(II) ion maintains its tetrahedral coordination, and the zinc-bound hydroxide interacts with the azetidinone ring via a C−H···O interaction. All levels of theory predict similar coordination geometries around the zinc(II) ion for the transition state (**2$_A$**) and the tetrahedral intermediate (**3$_A$**). Thus, the TS **2$_A$** corresponds to a tight five-coordinated zinc complex while the degraded β-lactam moiety in **3$_A$** is bound to the zinc(II) ion in an asymmetric bidentate manner with Zn−O and Zn−OH distances of ∼1.9 and ∼2.5 Å, respectively. Note that the zinc-(II) charge (+1.6 e, B3LYP, MP2; +1.7, HF) is quite similar in the **1$_A$**−**3$_A$** structures. In Figure 6 see that the MP4/6-31G*// MP2/6-31G* and MP2/6-31G* levels predict very similar relative energies (∼17−18 and ∼10 kcal/mol for the energy barrier and reaction energy, respectively). The inclusion of basis set effects at the MP2/6-311+G(2d,2p)/MP2/6-31G* level results in an energy barrier of 22.3 kcal/mol and a reaction energy of 14.4 kcal/mol. The B3LYP/6-31G* values (19.7 and 14.1 kcal/mol) are in satisfactory agreement with the MP2/6-311+G(2d,2p)//MP2/6-31G* results. The HF/6-31G* level predicts a reasonable energy barrier (21.0 kcal/mol), but underestimates the reaction energy by 2.3 kcal/mol with respect to MP2/6-311+G(2d,2p)/MP2/6-31G*.

In this study, we postulate that protonation of the leaving N atom in the hydrolysis of β-lactams may occur via proton transfer from the doubly protonated His210 residue. A similar chemical event can be modeled at high levels of theory in the related system imidazole + methylamine. In agreement with previous computational experience,[62] we found that correlation energy has a large influence on the energetics, charge distribution, and geometries of the **1$_B$**, **2$_B$**, and **3$_B$** critical structures involved in the $CH_3NH_3^+$ ↔ imidazole proton transfer (see Figure 7). For example, the equilibrium distances of the N···N

(61) Vahrenkamp, H. *Acc. Chem. Res.* **1999**, *32*, 589−596.

(62) Stanton, R. V.; Merz, K. M., Jr. *J. Chem. Phys.* **1994**, *101*, 6658−6665.

Table 4. Relative Energies (kcal/mol) of the Structures Involved in the Hydrolysis Reaction of *N*-Methyl-2-azetidinone and the Mononuclear Cluster Model of the *B. cereus* Active Site[a]

structures	PM3	HF/6-31G*//PM3	HF/6-31G*	$G_{thermal}$	B3LYP/6-31G*//HF/6-31G*	B3LYP/6-31G*
$\mathbf{1_D}$	0.0 (0.0)	0.0	0.0	0.0	0.0 (0.0)	0.0 (0.0)
$\mathbf{2_D}$ **(TS)**	19.2 (2.8)	16.8	22.7	2.8	17.2 (2.3)	17.0 (4.0)
$\mathbf{3_D}$	−9.2 (−1.4)	−1.0	−4.2	4.3	8.3 (−1.1)	
$\mathbf{4_D}$ **(TS)**	3.2 (4.1)	12.4	13.2	3.4	5.9 (5.9)	
$\mathbf{5_D}$	−41.9 (10.8)	−37.4	−39.9	4.5	−30.4 (4.4)	−28.6 (1.1)

[a] Relative solvation energies ($\Delta\Delta G_{solvation}$, in kcal/mol) are shown in parentheses as obtained from PM3 and B3LYP/6-31G* SCRF-PB calculations. Thermal corrections to Gibbs energies were obtained from the HF/3-21G* unscaled frequencies.

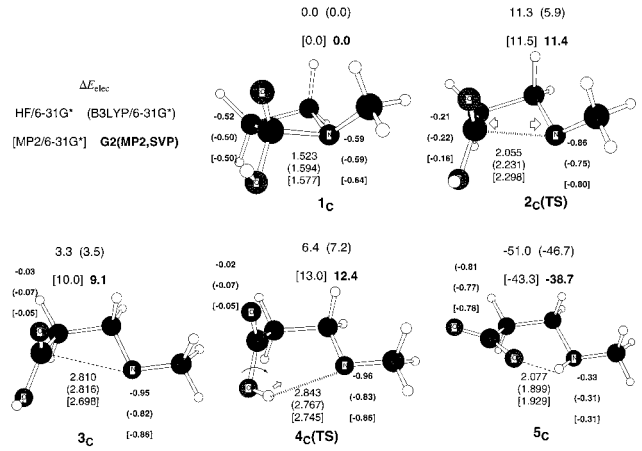

Figure 8. Optimized structures involved in the evolution of a tetrahedral intermediate during the alkaline hydrolysis of *N*-methylazetinone. Some significant distances (Å) and NPA charges are given at the HF/6-31G*, (B3LYP/6-31G*), and [MP2/6-31G*] levels of theory. Relative energies (kcal/mol) at different levels of theory are also indicated.

contacts at $\mathbf{1_B}$ and $\mathbf{3_B}$ are ∼0.1 Å shorter when correlation energy is included. B3LYP/6-31G* and the sophisticated G2(MP2,SVP) computational procedure predict a low energy barrier of ∼1.2 for proton transfer from the imidazole moiety to methylamine.[63] Moreover, inclusion of the B3LYP/6-31G* ZPVE correction (−1.9 kcal/mol) makes this energy difference vanish so that the $\mathbf{2_B}$ structure becomes a global minimum on the PES. The energetic cost associated with the proton-transfer event in model **B** is notably overestimated at HF/6-31G* (ΔE_{elec}= 6.4 kcal/mol).

To better understand the energetics of C−N bond cleavage in the hydrolysis of β-lactams, we studied the collapse of a tetrahedral intermediate potentially involved in the alkaline hydrolysis of *N*-methyl-2-azetidinone (see Figure 8). As observed in former theoretical work,[60,64] the ring opening of this kind of intermediate and proton transfer to the leaving amino group can take place asynchronously, that is, involving the participation of an unstable ring-opened species (see the sequence of structures $\mathbf{1_C} \rightarrow \mathbf{2_C} \rightarrow \mathbf{3_C} \rightarrow \mathbf{4_C} \rightarrow \mathbf{5_C}$ in Figure 8). Energetically, the barrier is determined by the cleavage of the C−N bond (11.4 kcal/mol at G2(MP2,SVP)). The process is highly exothermic with a reaction energy of −38.7 kcal/mol at G2(MP2,SVP). Note that B3LYP/6-31G* significantly underestimates the energy barrier required for C−N cleavage (5.5 kcal/mol lower than G2(MP2,SVP)).

Overall, we conclude that the levels of theory to be used for large systems (B3LYP/6-31G* and HF/6-31G*) can yield reasonable structures for the transition states and intermediates involved in the hydrolysis of β-lactams catalyzed by zinc-β-lactamases. Nevertheless, it is also clear that B3LYP/6-31G* gives a more balanced description for the energetics and geometries.

QM Enzymatic Model. Clearly, an examination of the more realistic model system **D** can provide valuable insight into the catalytic machinery of the mononuclear *B. cereus* enzyme. In this model, the zinc(II) ion is complexed by three methylimidazole ligands and includes the side chains of Asp90 and His210. Both HF/6-31G* and B3LYP/6-31G* levels, whose relative performance was assessed in the previous calculations, were used. All the structures were also optimized by using the PM3 method to compare between the ab initio and semiempirical structures and energies. To prevent movement of groups of atoms to locations unattainable in the actual *B. cereus* system, the Cβ atoms (methyl groups) were held fixed throughout the computations in the relative position found in the 1BME crystal structure.[14] We note, however, that the model is still reasonably flexible. The optimized structures are shown in Figure 9 while their relative energies are given in Table 4.

The optimized complex between the active site model and *N*-methyl-2-azetidinone ($\mathbf{1_D}$ in Figure 9) has residue−residue contacts and β-lactam−residue interactions which are quite similar to those found in the NAC complexes found in the MD simulation. Thus, the zinc-bound hydroxide interacts with both the Asp90 carboxylate group and the His210 imidazole through H-bond contacts. These important H-bonds are ∼0.1 Å shorter at the B3LYP/6-31G* level than at HF/6-31G* (see Figure 9). The carbonyl group of the β-lactam interacts with the zinc cluster via two CH···O contacts of 2.1−2.2 Å with the Cε1−Hε1 bonds of His88 and His149. To complement these structural observations, we analyzed the B3LYP/6-31G* charge density by locating and characterizing the bond critical points (BCP) for the zinc−ligand bonds and the relevant H-bond interactions (these results are shown in the Supporting Information). Most importantly, these analyses reveal the appearance of the Cε1−Hε1···O BCPs and the absence of BCP for a Zn···carbonyl interaction. This suggests that the tetrahedral environment around the zinc(II) ion is hardly distorted by the presence of the β-lactam moiety.

The $\mathbf{1_D}$ complex is connected to the transition state $\mathbf{2_D}$ located on the B3LYP/6-31G* and HF/6-31G* PES. In this TS, the attack of the zinc-bound hydroxide on the β-lactam carbonyl group appears favored by the presence of the Zn−OH···$^{-}$OCO−Asp90 linkage, which is slightly reinforced (shorter H-bond distance) with respect to $\mathbf{1_D}$. The forming C−O bond has an equilibrium distance of 1.859 and 2.040 Å at the HF/6-31G* and B3LYP/6-31G* levels, respectively (the HF/3-21G* transition vector is dominated by the C−O bond forming process). The computed energy barriers for $\mathbf{2_D}$ are 22.7 and 17.0 kcal/mol at HF/6-31G* and B3LYP/6-31G*, respectively, with respect to $\mathbf{1_D}$. The total charge transfer from the zinc-bound hydroxide to the β-lactam amounts to 0.14 e while the positive charge on the zinc(II) ion (1.78 e, HF; 1.65 e, B3LYP) is

(63) Gerlt, J. A.; Kreevoy, M. M.; Cleland, W. W.; Frey, P. A. *Chem. Biol.* **1997**, *4*, 259−267.

(64) Pitarch, J.; Ruiz-López, M. F.; Pascual-Ahuir, J. L.; Silla, E.; Tuñón, I. *J. Phys. Chem. B* **1997**, *101*, 3581−3588.

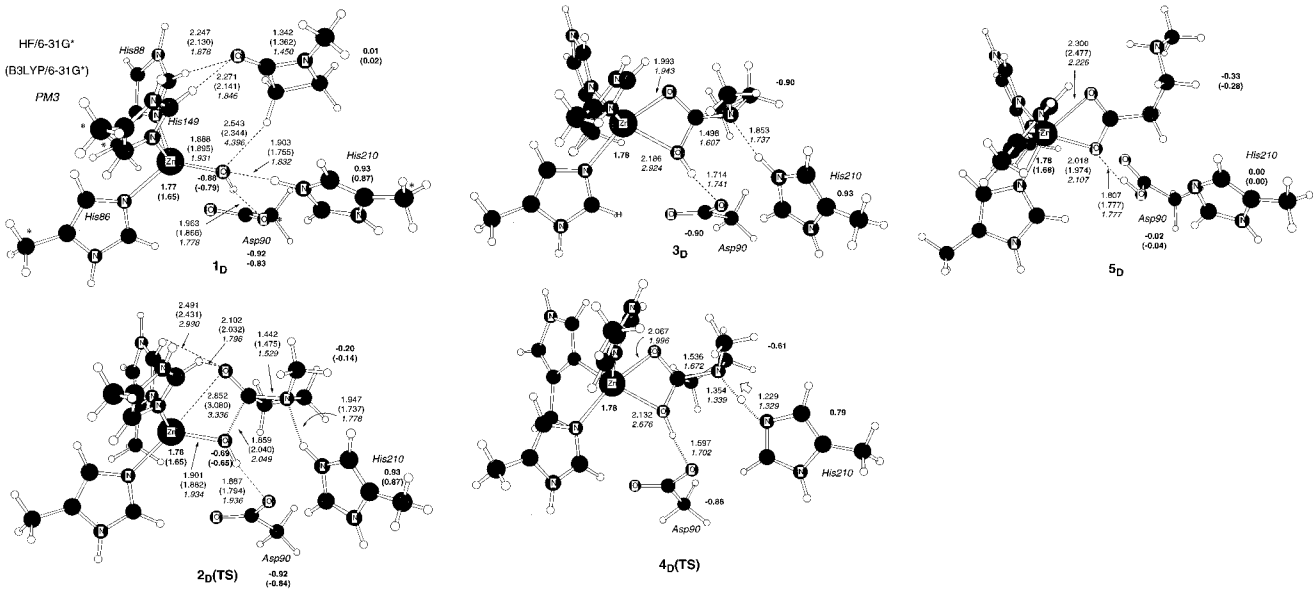

Figure 9. Optimized structures involved in the hydrolysis reaction of *N*-methylazetidinone with the $[Zn(methylimidazol)_3(OH)]^+$ complex in the presence of the Asp90 and His210 side chains. The C atoms in the methyl groups were held fixed at their X-ray equilibrium position. Some significant distances (Å) and NPA charges are given at the HF/6-31G* and (B3LYP/6-31G*) levels. PM3 data (in italics) are also indicated.

preserved with respect to $\mathbf{1_D}$. Interestingly, most of the charge transfer is accumulated on the endocyclic N atom (−0.10 and −0.12 e at HF and B3LYP) instead of the carbonyl oxygen atom, which is now 2.852 Å (HF) and 3.080 Å (B3LYP) away from the zinc(II) ion. The Cϵ1−Hϵ1···O contacts are still present and, therefore, it appears that both the zinc-ligands and the zinc ion stabilize the β-lactam carbonyl at the TS. The doubly protonated His210 residue establishes a strong Nϵ2−H···N contact with the β-lactam N atom, which is much stronger at the B3LYP/6-31G* level (1.737 Å) than at HF/6-31G* (1.947 Å). Analysis of the B3LYP/6-31G* charge density for $\mathbf{2_D}$ shows the presence of BCP for the reactive interactions (i.e., the forming C−O bond and the N−H···N contact), but no BCP was found between the zinc(II) ion and the carbonyl O atom of the β-lactam. Thus, the geometrical and electronic changes for the zinc coordination environment are only minor on going from $\mathbf{1_D}$ to the TS $\mathbf{2_D}$, that is, the required coordinative flexibility of the zinc(II) ion for catalysis[61] appears unimportant for nucleophilic attack in this case.

The structure of $\mathbf{2_D}$ suggests that this critical point is only a TS for nucleophilic attack at the HF/6-31G* level and is a TS for *both* nucleophilic attack and proton transfer at B3LYP/6-31G*. This was confirmed by the appearance of the HF/6-31G* critical structures $\mathbf{3_D}$ and $\mathbf{4_D}$ and their absence on the B3LYP/6-31G* PES. Nevertheless, the characterization of $\mathbf{3_D}$ and $\mathbf{4_D}$ generates some interesting mechanistic details. Thus, $\mathbf{3_D}$ corresponds to a tetrahedral intermediate that binds to zinc(II) in a bidentate manner while the β-lactam ring remains intact. The unprotonated N atom of the β-lactam ring has an H-bond with the Nϵ2−Hϵ2 bond of His210 (1.853 Å). Energetically, $\mathbf{3_D}$ is quite stable at the HF/6-31G* level since it is 4.2 kcal/mol below the prereactive complex $\mathbf{1_D}$. There is a notable energy barrier (17.4 kcal/mol with respect to $\mathbf{3_D}$) for the His210→β-lactam proton transfer through the HF/6-31G* TS structure $\mathbf{4_D}$.

Single-point B3LYP/6-31G*//HF/6-31G* calculations reflect dramatic changes in the $\mathbf{2_D} \rightarrow \mathbf{3_D} \rightarrow \mathbf{4_D}$ energy profile: $\mathbf{3_D}$ turns out to be 2.4 kcal/mol less stable than $\mathbf{4_D}$, that is, completion of the His210→β-lactam proton transfer is a barrierless process when correlation energy is included. On the other hand, according to the B3LYP/6-31G*//HF/6-31G* solvation energies, the tetrahedral intermediate $\mathbf{3_D}$ could be relatively stable in a highly polar environment since the $\Delta\Delta G_{solvation}$ values indicate that solvent effects disfavor the proton-transfer TS $\mathbf{4_D}$ by 7.0 kcal/mol with respect to $\mathbf{3_D}$. Nonetheless, all the calculations clearly indicate that the TS structure $\mathbf{2_D}$ is the rate-determining step both in vacuo and in the solvent continuum (see Table 4).

The rupture of the β-lactam C−N bond through a stretching motion is required to form the hydrolysis product complex and to ultimately release the product. According to our calculations, this process takes place after protonation of the N atom and does not involve an energy barrier: no critical point for the C−N rupture was found either on the HF/6-31G* PES or on the B3LYP/6-31G* PES. In fact, the rupture of the C−N bond is greatly favored by the release of the β-lactam ring strain energy during the later stages of the process (ca. −30 kcal/mol for azetidinones).[65] In agreement with this, the calculated energy of the product complex ($\mathbf{5_D}$ in Figure 9) is −39.9 and −28.6 kcal/mol at HF/6-31G* and B3LYP/6-31G* levels, with respect to $\mathbf{1_D}$. In the cluster model **D**, elongation of the C−N bond is accompanied by proton transfer from the zinc-bound hydroxide to the carboxylate of Asp90. Thus, the newly formed carboxylate group of the degraded β-lactam and the zinc(II) ion form a bidentate adduct (see Figure 9). Nevertheless, we expect that the actual charge distribution of the final product complex and the mechanism for product release would be largely influenced by the protein and solvent environments.

PM3 energies and some equilibrium distances are shown in Table 4 and Figure 9, respectively. We used a new set of PM3 parameters for Zn developed in our laboratory.[55] These parameters give Mulliken charges on the Zn atom (∼ +0.7) which compare well with the ab initio ones (∼ +0.8) and are more realistic than those provided by the original parameters (∼ +0.05). The PM3 relative energies also compare well with the HF/6-31G* values and single-point HF/6-31G*//PM3 calculations give energetic trends, which generally coincide with those of HF/6-31G*. The PM3 method gives coordination geometries around the zinc ion that are quite similar to those of the HF/6-31G*

(65) Roux, M. V.; Jiménez, P.; Dávalos, J. Z.; Castaño, O.; Molina, M. T.; Notario, R.; Herreros, M.; Abboud, J.-L. M. *J. Am. Chem. Soc.* **1996**, *118,* 12735−12737.

structures, except for the intermediate $\mathbf{3_D}$ in which PM3 predicts the Zn ion to bind the carboxylate in a monodentate fashion instead of the bidentate mode of binding predicted by HF/6-31G*. However, previous theoretical work has shown that the energy difference between monodentate and bidentate coordination of carboxylate groups to zinc ions is not large (<5 kcal/mol).[66] Of particular interest are the structure and energetics for the rate-determining TS $\mathbf{2_D}$. We see that all the levels of theory give a similar description for this important structure (i.e., a *reactant-like* character and a moderate energy barrier of ~17−23 kcal/mol). This observation suggests that the structure of this important TS is invariant with respect to the level of theory and that semiempirical methods could be used to treat larger systems.

Comparison with the Alkaline Hydrolysis of β-Lactams. By combining the B3LYP/6-31G* energy barrier for the rate-determining TS for the QM enzymatic model ($\mathbf{2_D}$) with thermal corrections and solvent continuum effects, we obtain ΔG barriers of 19.8 and 23.8 kcal/mol in vacuo and in the continuum, respectively. To obtain further insight into the enzymatic process, the $\Delta G_{solution}$ barrier for a reference reaction in solution was also examined computationally. The alkaline hydrolysis of 3α-carboxypenam was chosen as a reference system (model **E** in Scheme 3) and the transition structure for hydroxide addition to the β-lactam carbonyl, which is the rate-determining step for the hydrolysis of all β-lactam antibiotics,[67] was optimized at the B3LYP/6-31+G* level (see Supporting Information). The estimated $\Delta G_{solution}$ barrier for this system was 31.4 kcal/mol. Because of the different nature of the model systems **D** and **E** and the levels of theory employed, the comparison between their energy barriers should be made with care. Nevertheless, these calculations suggest that the enzymatic system could give a barrier reduction of several kilocalories per mole with respect to the hydroxide ion catalyzed process. This is in consonance with the experimentally observed 10^6-fold rate enhancement for the class B β-lactamase from *B. cereus*.[68]

Docking of the QM Enzymatic Model in the *B. cereus* Enzyme. To assess the structural viability of the catalytic mechanism facilitated by the His210 side chain, we built a model of the rate-determining transition structure $\mathbf{2_D}$ embedded in the active site region of the *B. cereus* enzyme. A single MD snapshot of the NAC complexes was chosen as the starting configuration in the model building. Then, the force field representing the **ZnOH-BP** configuration was modified to model the transition state (e.g., the C7 and N4 BP atoms were linked to the O−Zn and Hε2@His210 atoms, respectively; see Supporting Information). The corresponding equilibrium bond lengths and bond angles were taken as the B3LYP/6-31G* optimized values in the $\mathbf{2_D}$ structure. The position of BP, the zinc complex, the most important residues (Asp90, Cys168, His210, Asn180, Lys171, Phe34, Val39, Trp59, etc.), and a solvent cap of 1500 water molecules centered on the zinc(II) ion were relaxed via MM energy minimization. This minimization led to the model **TS(ZnOH-BP)** shown in Figure 10. From **TS(ZnOH-BP)**, a prereactive complex **C(ZnOH-BP)** was also obtained by energy minimization, using the original **ZnOH-BP** force field representation. Finally, the energy of the **TS-(ZnOH-BP)** and **C(ZnOH-BP)** MM models was evaluated by using PM3 D&C calculations following the computational procedure described in the Methods section.

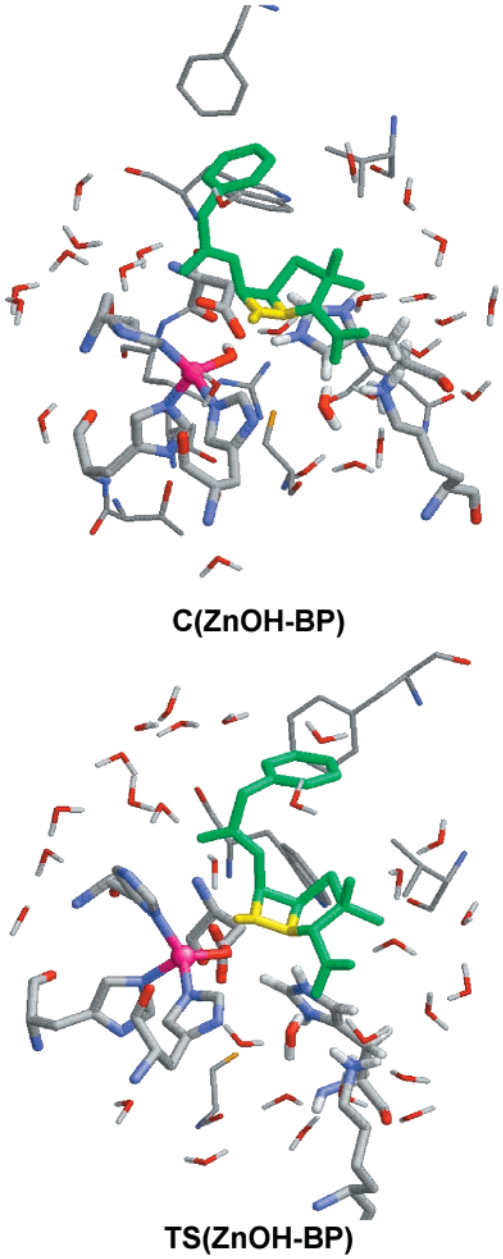

Figure 10. MM models of the prereactive complex and the TS for the His210-assisted hydrolysis of BP catalyzed by the *B. cereus* enzyme (see text for details).

The docked structure **TS(ZnOH-BP)** shown in Figure 10 confirms that the zinc-bound hydroxide can attack the BP carbonyl group in an orientation such that the enzyme−substrate interactions are still present at the TS configuration. With respect to the prereactive configuration **C(ZnOH-BP)**, the H-bond between the NH backbone of Asn180 and the β-lactam carbonyl was the only interaction that was substantially weakened at **TS-(ZnOH-BP)**. Also, we note that the partial flipping of the His210 side chain required to reach **TS(ZnOH-BP)** is sterically allowable. Other residues, like Cys168 and Asp90, are nearly unaffected. In terms of their PM3 energies ($E_{PM3-D\&C}$), the **TS-(ZnOH-BP)** configuration is 18.5 kcal/mol less stable than **C-(ZnOH-BP)**. Note that this energy difference is quite similar to the PM3 barrier, 19.2 kcal/mol, obtained for the cluster model **D** (see Table 4). The effect of bulk solvent was taken into account by means of PM3 D&C PB calculations which gave a $\Delta\Delta G_{solvation}$ value of only −0.9 kcal/mol favoring the transition

(66) Ryde, U. *Biophys. J.* **1999**, *77*, 2777−2787.
(67) Page, M. I. *The mechanisms of reactions of β-lactams*; Page, M. I., Ed.; Blackie Academic&Professional: London, 1992; pp 129−147.
(68) Laws, A. P.; Page, M. I. *J. Chem. Soc., Perkin Trans. 2* **1989**, 1577−1581.

state configuration in contrast with the solvent continuum effect observed in the QM cluster model (see above).

To estimate the influence of higher levels of theory in the energetic description of the catalytic machinery of the *B. cereus* enzyme, we performed single-point B3LYP/6-31G* ($E_{B3LYP6-31G*}$) and standard PM3 (E_{PM3}) calculations on subsystems of **TS-(ZnOH-BP)** and **C(ZnOH-BP)**. These subsystems consisted of the BP substrate, the zinc(II) cation, and the side chains of His86, His88, Asp90, His149, Cys168, and His210 (H-link atoms were attached to the corresponding Cβ atoms). The computed value for the energy difference, $\Delta E_{B3LYP/6-31+G*} - \Delta E_{PM3} = +5.9$ kcal/mol, can be seen as a high level correction to the global energies (ΔE). The different energy terms can be combined in the following manner:

$$\Delta E \approx \Delta E_{PM3-D\&C} + \Delta\Delta G_{solvation} + [\Delta E_{B3LYP/6-31G*} - \Delta E_{PM3}] \quad (2)$$

The resultant ΔE for the solvated protein amounts to 23.8 kcal/mol. Comparison of this energy barrier with those obtained at the different levels of theory for the cluster model **D** (~17−23 kcalmol) suggests that the residues considered in the cluster model incorporate all of the essential catalytic machinery of the *B. cereus* enzyme. However, these energy calculations on the MM models should be considered as an upper limit to the enzymatic energy barrier: a full relaxation of the TS model and/or calculation of the whole reaction path in the enzyme would be necessary to provide a more accurate energy profile. Moreover, further catalytic advantage may come from entropic contributions arising from the structural elasticity of the protein environment.

Discussion

Knowledge gained on the structure and dynamics of the mononuclear zinc-β-lactamase from *B. cereus* can be combined with the results obtained in the QM study of the hydrolysis process to outline a global catalytic cycle (see Scheme 4).

According to the QM/MM calculations reported in our previous article,[22] the energy difference between the **ZnOH** and **ZnOH$_2$** configurations representing the free form of the enzyme has a magnitude similar to the fluctuations of their individual energies. Thus, both states could be appreciably populated and subject to rapid interconversion given that, for example, a Zn−OH$_2$→Nϵ2@His210 proton-transfer process from the **ZnOH$_2$** state may readily occur through a water-assisted pathway with an estimated barrier of ~8 kcal/mol.[22] Since the **ZnOH** configuration has a partially desolvated and properly oriented *hard* nucleophile in the form of the zinc-bound hydroxide moiety, this configuration should correspond to the kinetically active configuration of the *B. cereus* enzyme. In agreement with mutagenesis experiments,[20,21,23] our MD simulations emphasize the critical role played by Asp90, His210, and Cys168 in stabilizing the **ZnOH** state. For example, the absence of the thiol group in the Cys168 mutants would imply the loss of the Sγ−Hγ···O−Zn interaction and, therefore, the population of the mutant *B. cereus* molecules that have the correct **ZnOH** configuration for catalysis would be substantially reduced with respect to the wild-type enzyme.

The MD simulation of the **ZnOH** model complexed with benzylpenicillin confirms some of the previous proposals about substrate-binding[15] and gives new insight into the nature of the enzyme−substrate binding determinants. These results highlight the important role of the conserved residues Asn180 and Lys171 as well as that of the hydrophobic Phe34, Val39, and Trp59

Scheme 4

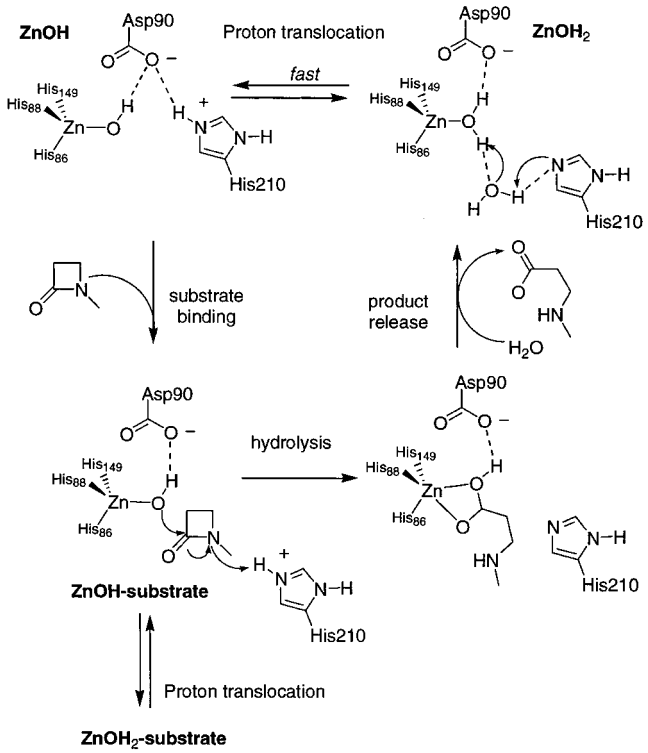

residues. Moreover, the structure and dynamics of the Michaelis complex suggest that the **ZnOH-BP** configuration could undergo a Nϵ2−Hϵ2@His210→O−Zn proton translocation since both groups establish a direct H-bond interaction in ~50% of the analyzed snapshots. This process could lead to a hypothetical **ZnOH$_2$-BP** configuration as depicted in Scheme 4. Reversion to the kinetically active state, **ZnOH-BP**, could occur through a water-assisted Zn−OH$_2$→Nϵ2@His210 proton transfer. The "deep" water molecule trapped in the vicinity of the zinc-bound hydroxide could be involved in this latter process. Therefore, the MD results reported on the **ZnOH-BP** model give further support to our former proposal that a rapid interconversion process between the **ZnOH** and **ZnOH$_2$** configurations in the presence of substrate could exist.[22] This hypothesis explains the existence of branched pathways that comprise conformationally distinct complexes as experimentally observed under cryoenzymological conditions.[18]

In our mechanistic proposal, the **ZnOH-BP** system hydrolyzes the β-lactam substrate by attack of the zinc-bound hydroxide ion with a concomitant proton transfer from the doubly protonated His210 residue to the leaving amino group. Overall, our calculations on the His210-assisted mechanism are in agreement with the experimental kinetic data for the monozinc form of the *B. cereus* enzyme. Thus, the proposed qualitative pK_a assignments in the Zn−OH···Asp90···His210 "triad", a high pK_a value for His210 and a relatively low pK_a for the Zn−OH···Asp90 pair with *two* proton acceptor sites,[22] are compatible with the experimental rate controlling ionization constants $pK_{a,1} = pK_{a,2}$ and $pK_{a,3}$ which have values of 5.6 and 9.5, respectively.[19] The structure of the rate-determining TS model is also compatible with the experimental kinetic isotope effects on the k_{cat}/K_m ratio (e.g., 1.82 for benzylpenicillin and 0.85 for cephalorodine).[19] Although the atomic motions of the transition vector for the cluster model are dominated by covalent chemistry (i.e., formation of the C−O bond), the strong Nϵ2−Hϵ2···N contact also suggests that a certain contribution of the His210→β-lactam proton transfer to the transition vector should be

expected. This is consistent with the small kinetic isotope effects which in turn can be modulated by the β-lactam substrates as they influence the strength of the Nε2−Hε2···N(β-lactam) interaction. On the other hand, the computed energy barriers for the MM model and the docked model of the rate-determining TS (17−24 kcal/mol) are in good agreement with the apparent energies of activation obtained from k_{cat}/K_M values (∼15 kcal/mol).[18] Clearly, prediction of a more accurate barrier would require the calculation of the total free energy change associated with the reaction process. Nevertheless, on the basis of the present results we conclude that the catalytic mechanism for the hydrolysis of β-lactams in which the zinc-bound hydroxide and the protonated His210 residue act as nucleophile and proton donor, respectively, is structurally and energetically feasible and is in agreement with the available experimental data.

For the *binuclear* zinc-β-lactamase from *B. fragilis*, spectroscopic studies have revealed the existence of an intermediate that has a negatively charged nitrogen leaving group and a cleaved β-lactam ring.[69] Interestingly, a similar intermediate also has been characterized in the hydrolysis of nitrocefin by a dizinc β-lactamase model complex.[70] In contrast, there is no experimental evidence supporting the existence of intermediates in the hydrolysis of β-lactams by the mononuclear *B. cereus* enzyme. This is in agreement with the B3LYP/6-31G* and B3LYP/6-31G*//HF/6-31G* calculations on the large cluster model which predict that tetrahedral intermediates are not stable species along the reaction profile. The fact that B3LYP/6-31G* may underestimate the energetic cost associated with the cleavage of the C−N bond and that a highly polar environment can destabilize the proton transfer to the leaving N atom suggest that a tetrahedral intermediate might actually appear on the PES. However, it is also true that the azetidinone model system is a β-lactam with a worse leaving group than that of most of the β-lactam antibiotics.[71] With all things taken into consideration, we expect that a tetrahedral intermediate would not accumulate to an experimentally detectable amount. This is because its formation via the initial nucleophilic attack would be the rate-determining step and the subsequent completion of the proton transfer to the leaving amino group and the rupture of the endocyclic C−N bond would be much faster.

Finally, we comment on the potential catalytic activity of the **$ZnOH_2$** form of the mononuclear *B. cereus* enzyme. In this model, the essential zinc(II) ion binds an undissociated water molecule with limited nucleophilic character.[22] From our molecular simulations of the wild-type enzyme, we have proposed that the **$ZnOH_2$** configuration would be the predominant one for the Cys168→Ser and His210→Met mutants. These *B. cereus* mutants have catalytic activities of less than 1−10% of that of the wild-type enzyme.[20,21] So, how might these mutant enzymes retain a low level of activity? The "deep" water molecule linking the β-lactam carboxylate and the zinc center during the **ZnOH-BP** simulation could occupy a similar position in a hypothetical **$ZnOH_2$-BP** model, suggesting an active catalytic role for this water molecule. In these mutants, we propose that the auxiliary water and the β-lactam carboxylate group would participate in a proton relay pathway from the Zn−OH_2 moiety to the leaving N atom during the hydrolysis process. A similar proposal has been recently reported for the acylation step in class-A β-lactamases.[72,73]

Acknowledgment. We would like to thank the NIH for supporting this research through Grant GM44974. We also thank the National Center for Supercomputer Applications for generous allocations of supercomputer time. N.D. and D.S. acknowledge MEC (Spain) for partial support of this work via grants PB98-44430549 and EX99-10863995Z.

Supporting Information Available: Optimized geometry, RESP HF/6-31G* atomic charges, and AMBER atom types for benzylpenicillin; tables containing a summary of RMSD-RMSF values; tables including the B3LYP/6-31G* BCP properties for the $\mathbf{1_D}$ and $\mathbf{2_D}$ models; a figure showing the TS structure for the alkaline hydrolysis of 3α-carboxypenam; a list of added force constants used to construct the **TS(ZnOH-BP)** model; and Cartesian coordinates for all the critical structures of model **D** (PDF). This material is available free of charge via the Internet at http://pubs.acs.org.

JA0113246

(69) Wang, Z.; Fast, W.; Benkovic, S. J. *Biochemistry* **1999**, *38*, 10013−10023.

(70) Kaminskaia, N. V.; Spingler, B.; Lippard, S. J. *J. Am. Chem. Soc.* **2001**, *123*, 6555−6563.

(71) Page, M. I. *Structure−activity relationships: chemical*; Page, M. I., Ed.; Blackie Academic&Professional: London, 1992; pp 79−100.

(72) Díaz, N.; Suárez, D.; Sordo, T. L.; Merz, K. M., Jr. *J. Phys. Chem. B.* In press.

(73) Atanasov, B.; Mustafi, D.; Makinen, M. W. *Proc. Natl. Acad. Sci* **2000**, *97*, 3160−3165.